

Warm stellar matter with deconfinement: application to compact stars

D.P.Menezes¹ and C. Providência²

¹*Depto de Física - CFM - Universidade Federal de Santa Catarina Florianópolis - SC - CP. 476 - CEP 88.040 - 900 - Brazil*

²*Centro de Física Teórica - Dep. de Física - Universidade de Coimbra - P-3004 - 516 Coimbra - Portugal*

We investigate the properties of mixed stars formed by hadronic and quark matter in β -equilibrium described by appropriate equations of state (EOS) in the framework of relativistic mean-field theory. We use the non-linear Walecka model for the hadron matter and the MIT Bag and the Nambu-Jona-Lasinio models for the quark matter. The phase transition to a deconfined quark phase is investigated. In particular, we study the dependence of the onset of a mixed phase and a pure quark phase on the hyperon couplings, quark model and properties of the hadronic model. We calculate the strangeness fraction with baryonic density for the different EOS. With the NJL model the strangeness content in the mixed phase decreases. The calculations were performed for $T = 0$ and for finite temperatures in order to describe neutron and proto-neutron stars. The star properties are discussed. Both the Bag model and the NJL model predict a mixed phase in the interior of the star. Maximum allowed masses for proto-neutron stars are larger for the NJL model ($\sim 1.9 M_{\odot}$) than for the Bag model ($\sim 1.6 M_{\odot}$).

PACS number(s): 21.65.+f, 21.30.-x, 95.30.Tg

I. INTRODUCTION

Landau predicted the possible existence of a neutron star after the neutrons were discovered by Chadwick in 1932. In 1934, it was suggested that neutron stars were formed after a supernova explosion, which happens when the core of a very massive star undergoes gravitational collapse. The first supernova explosion was registered in 1054 by the Chinese. The Crab Nebula in the Taurus constellation is the remnant of this explosion. Recently, a supernova explosion was observed in the Magellanic Cloud 170,000 light years from the Earth. Once the gravitational collapse of a massive star with mass of the order or larger than 8 solar masses takes place, a proto-neutron star can be formed. Several different stages may happen during the evolution process [1, 2]. The proto-neutron stars are known as evolutionary endpoints and they slowly cool down to form a neutron star, which is a stable and cold compact star. The structure of compact stars is characterized by its mass and radius, which in turn are obtained from appropriate equations of state (EOS) at densities about one order of magnitude higher than those observed in ordinary nuclei. At these densities, relativistic effects are certainly important.

In this work we investigate the equation of state (EOS) of warm, β -equilibrium hadron/quark matter and apply it to determine the properties of mixed stars consisting of hadron matter with hyperons and quark matter. In particular we investigate the mixed phase with hadron and quark matter and search for the possibility of existence of a pure quark matter core inside compact stars. The calculations are performed for finite and zero temperature in order to describe proto-neutron and neutron stars, respectively. We consider only the phase after deleptonization, when neutrinos have already diffused out.

For hadron matter the relativistic non linear Walecka model [3, 4] with the inclusion of the baryonic octet is used. For sufficiently high densities it is expected that the formation of hyperons in a neutron star is energetically favored. Experimental constraints obtained from hyper-nuclei give estimates of the hyperon-nucleon and hyperon-hyperon interactions, which impose restrictions on the expected properties of neutron stars [5]. The appearance of the strange-baryons softens the EOS and lowers the maximum mass of a stable neutron star [5]. Another possible source of softening of the EOS is the onset of quark matter. According to the hyperon couplings and the properties of the quark model, this may occur for densities lower or higher than the one corresponding to the onset of hyperons [1]. For quark matter, the MIT Bag model [6] and the Nambu-Jona-Lasinio model [7] with three quark flavors were chosen. The NJL model contains some of the basic symmetries of QCD, namely chiral symmetry. It has been very successful in describing the low lying mesons and predicts at sufficiently high densities/temperatures a phase transition to a chiral symmetric state [8, 9, 10, 11]. However, it is just an effective theory that does not take into account quark confinement. This rises no problems because we only use the NJL model to describe the deconfined phase. At sufficiently large baryonic densities the quark structure of the hadrons gives rise to a phase transition into quark matter. This conversion takes place at densities a few times the nuclear matter density [5]. The Gibb's criteria are enforced in obtaining the coexistence phase. We also check whether the existence of the phase transition depends on

the choice of parameters for both hadron and quark matter equations of state, as pointed out in [12]. The complete EOS is built from the hadronic EOS at small densities, the mixed EOS for intermediate densities and a quark matter EOS for higher densities.

One of the aims of the present work is to understand the importance of chiral symmetry for the description of the quark matter. There have been contradictory results presented using the NJL model [13, 14], namely with respect to the possibility of existing a mixed phase of hadrons and quarks inside a neutron star. We also study the role of the hyperon coupling constants in the appearance of the phase transition to quark matter and the change of strangeness composition with density. Mixed star properties are obtained by solving the appropriate equations for temperatures up to 30 MeV.

The present paper is organized as follows: in section II both models used for the quark matter are described and in section III the non linear Walecka model with hyperons is reviewed. In both sections the conditions for beta equilibrium and charge neutrality are discussed. In section IV the mixed phase is implemented, the results are shown and discussed and in section V the properties of compact stars are computed. Finally, in the last section, the conclusions are drawn.

II. QUARK MATTER EQUATION OF STATE

A. The Nambu-Jona-Lasinio Model

We describe the quark phase within a model with chiral symmetry, the SU(3) NJL model which includes scalar-pseudoscalar and the 't Hooft six fermion interaction that models the axial $U(1)_A$ symmetry breaking. The NJL model [8, 9, 10, 11] is defined by the Lagrangian density

$$L = \bar{q}(i\gamma^\mu \partial_\mu - m)q + g_S \sum_{a=0}^8 [(\bar{q}\lambda^a q)^2 + (\bar{q}i\gamma_5 \lambda^a q)^2] + g_D \{ \det [\bar{q}_i(1 + \gamma_5)q_j] + \det [\bar{q}_i(1 - \gamma_5)q_j] \}, \quad (1)$$

where $q = (u, d, s)$ are the quark fields and λ_a ($0 \leq a \leq 8$) are the U(3) flavor matrices. The model parameters are: $m = \text{diag}(m_u, m_d, m_s)$, the current quark mass matrix ($m_d = m_u$), the coupling constants g_S and g_D and the cutoff in three-momentum space, Λ .

The set of parameters is chosen in order to fit the values in vacuum for the pion mass, the pion decay constant, the kaon mass and the quark condensates. We consider the set of parameters [11, 15]: $\Lambda = 631.4$ MeV, $g_S \Lambda^2 = 1.824$, $g_D \Lambda^5 = -9.4$, $m_u = m_d = 5.6$ MeV and $m_s = 135.6$ MeV which were fitted to the following properties: $m_\pi = 139$ MeV, $f_\pi = 93.0$ MeV, $m_K = 495.7$ MeV, $f_K = 98.9$ MeV, $\langle \bar{u}u \rangle = \langle \bar{d}d \rangle = -(246.7 \text{ MeV})^3$ and $\langle \bar{s}s \rangle = -(266.9 \text{ MeV})^3$. The frequently used set $\Lambda = 602.3$ MeV, $g_S \Lambda^2 = 1.835$, $g_D \Lambda^5 = -12.36$, $m_u = m_d = 5.5$ MeV and $m_s = 140.7$ MeV [16] gives similar results but since it has a smaller cut-off and we want to study quark matter at high densities we have preferred the first set.

The thermodynamical potential density is given by $\Omega = \mathcal{E} - TS - \sum_i \mu_i N_i - \Omega_0$, where the energy density is

$$\mathcal{E} = -2N_c \sum_i \int \frac{d^3p}{(2\pi)^3} \frac{p^2 + m_i M_i}{E_i} (n_{i-} - n_{i+}) \theta(\Lambda^2 - p^2) - 2g_S \sum_{i=u,d,s} \langle \bar{q}_i q_i \rangle^2 - 2g_D \langle \bar{u}u \rangle \langle \bar{d}d \rangle \langle \bar{s}s \rangle - \mathcal{E}_0 \quad (2)$$

and the entropy density is

$$S = -2N_c \sum_{i=u,d,s} \int \frac{d^3p}{(2\pi)^3} \theta(\Lambda^2 - p^2) \{ [n_{i+} \ln(n_{i+}) + (1 - n_{i+}) \ln(1 - n_{i+})] + [n_{i+} \rightarrow n_{i-}] \}. \quad (3)$$

In the above expressions $N_c = 3$, T is the temperature, μ_i (N_i) is the chemical potential (number) of particles of type i , and \mathcal{E}_0 and Ω_0 are included in order to ensure $\mathcal{E} = \Omega = 0$ in the vacuum. This requirement fixes the density independent part of the EOS. The ground-state of the system is described by the density matrix [11] given by $f = \text{diag}(f_u, f_d, f_s)$ with

$$f_i = \frac{1}{2} [I(n_{i-} + n_{i+}) - \frac{\gamma^0 M_i + \boldsymbol{\alpha} \cdot \mathbf{p}}{E_i} (n_{i-} - n_{i+})] \theta(\Lambda^2 - p^2), \quad (4)$$

where I is the identity matrix, $n_i^{(\mp)}$ are the Fermi distribution functions of the negative (positive) energy states, $n_i^{(\mp)} = [1 + \exp(\mp(\beta(E_i \pm \mu_i)))]^{-1}$, $i = u, d, s$. In the last equation $\beta = 1/T$, M_i is the constituent quark mass, $E_i = (p^2 + M_i^2)^{1/2}$.

The quark condensates and the quark densities are defined, for each one of the flavors $i = u, d, s$, respectively as:

$$\langle \bar{q}_i q_i \rangle = -2N_c \int \frac{d^3p}{(2\pi)^3} \frac{M_i}{E_i} (n_{i-} - n_{i+}) \theta(\Lambda^2 - p^2), \quad (5)$$

$$\rho_i = \langle q_i^\dagger q_i \rangle = 2N_c \int \frac{d^3p}{(2\pi)^3} (n_{i-} + n_{i+} - 1) \theta(\Lambda^2 - p^2). \quad (6)$$

Minimizing the thermodynamical potential Ω with respect to the constituent quark masses M_i leads to three gap equations for the masses M_i

$$M_i = m_i - 4g_S \langle \bar{q}_i q_i \rangle - 2g_D \langle \bar{q}_j q_j \rangle \langle \bar{q}_k q_k \rangle, \quad (7)$$

and cyclic permutations of i, j, k .

We introduce an effective dynamical Bag pressure [13, 17],

$$\begin{aligned} B = & 2N_c \sum_{i=u,d,s} \int \frac{d^3p}{(2\pi)^3} \left(\sqrt{p^2 + M_i} - \sqrt{p^2 + m_i} \right) \theta(\Lambda^2 - p^2) \\ & - 2g_S \sum_{i=u,d,s} \langle \bar{q}_i q_i \rangle^2 - 4g_D \langle \bar{u} u \rangle \langle \bar{d} d \rangle \langle \bar{s} s \rangle. \end{aligned}$$

In terms of this quantity the energy density (2) takes the form

$$\mathcal{E} = 2N_c \sum_{i=u,d,s} \int \frac{d^3p}{(2\pi)^3} \sqrt{p^2 + M_i} (n_{i+} - n_{i-} + 1) \theta(\Lambda^2 - p^2) + B_{eff}, \quad B_{eff} = B_0 - B, \quad (8)$$

where $B_0 = B_{\rho_u=\rho_d=\rho_s=0}$. Writing the energy density in terms of B_{eff} allows us to identify this contribution as a Bag pressure and establish a relation with the MIT Bag model [7, 17] discussed in the next section.

We point out that the NJL model is only valid to describe the quark phase as far as the momenta of the quarks are smaller than the momentum cut-off Λ .

B. The MIT Bag Model

Quark matter has been extensively described by the MIT Bag model [6]. In its simplest form, the quarks are considered to be free inside a Bag and the thermodynamic properties are derived from the Fermi gas model. The energy density, the pressure and the quark q density are respectively given by:

$$\mathcal{E} = 3 \times 2 \sum_{q=u,d,s} \int \frac{d^3p}{(2\pi)^3} \sqrt{\mathbf{p}^2 + m_q^2} (f_{q+} + f_{q-}) + Bag, \quad (9)$$

$$P = \frac{2}{\pi^2} \sum_q \int dp \frac{\mathbf{p}^4}{\sqrt{\mathbf{p}^2 + m_q^2}} (f_{q+} + f_{q-}) - Bag, \quad (10)$$

$$\rho_q = 3 \times 2 \int \frac{d^3p}{(2\pi)^3} (f_{q+} - f_{q-}), \quad (11)$$

where 3 stands for the number of colors, 2 for the spin degeneracy, m_q for the quark masses, Bag represents the bag pressure and the distribution functions for the quarks and anti-quarks are the Fermi distributions

$$f_{q\pm} = 1/(1 + \exp[(\epsilon \mp \mu_q)/T]), \quad (12)$$

with μ_q being the chemical potential for quarks and anti-quarks of type q and $\epsilon = \sqrt{\mathbf{p}^2 + m_q^2}$. These equations were obtained for finite temperatures. For $T = 0$, the expressions can be read off the above ones by eliminating the antiparticles and substituting the particle distribution functions by the usual step functions.

We have used $m_u = m_d = 5.5$ MeV, $m_s = 150.0$ MeV and $Bag = (180 \text{ MeV})^4$ or $Bag = (190 \text{ MeV})^4$. If m_u , m_d and m_s are chosen as in the NJL model, the behavior of the properties of interest are not altered, since they are more dependent on the Bag pressure than on small differences in the quark masses.

C. Quark matter in beta equilibrium

In a star with quark matter we must impose both beta equilibrium and charge neutrality [5]. We consider the stage after deleptonization when entropy is maximum and neutrinos diffuse out. In this case the neutrino chemical potential is zero. For β -equilibrium matter we must add the contribution of the leptons as free Fermi gases (electrons and muons) to the energy and pressure. The relations between the chemical potentials of the different particles are given by

$$\mu_s = \mu_d = \mu_u + \mu_e, \quad \mu_e = \mu_\mu. \quad (13)$$

For charge neutrality we must impose

$$\rho_e + \rho_\mu = \frac{1}{3}(2\rho_u - \rho_d - \rho_s).$$

For the electron and muon densities we have

$$\rho_l = 2 \int \frac{d^3p}{(2\pi)^3} (f_{l+} - f_{l-}), \quad l = e, \mu \quad (14)$$

where the distribution functions for the leptons are given in eq.(12) by substituting q by l , with μ_l as the chemical potential for leptons of type l . At $T = 0$, equation (14) becomes simply $\rho_l = k_{Fl}^3/3\pi^2$.

In figure 1 we plot the effective bag pressure B_{eff} for several temperatures and for quark matter in beta equilibrium. As discussed in [13] for $T = 0$ MeV around 161-163 MeV there is a plateau between $\rho = 3\rho_0$ and $5\rho_0$. This corresponds to partial chiral symmetry restoration for quarks u and d but the chemical potential for quarks s , μ_s , is still lower than m_s . For higher densities, $\mu_s > m_s$ and the mass of the quark s goes slowly to its current quark mass value as density increases. For high densities, if the current quark masses were zero, the bag pressure $B \rightarrow 0$ and the quarks would behave as a gas of massless non-interacting particles inside a large MIT Bag with a bag constant B_0 [17]. At finite temperature, the value 161 MeV is only reached at higher densities and the plateau slowly disappears. This behavior is due to the fact that the mass of the quarks decrease slower with ρ and the quark s exists for $\mu_s < m_s$. In fig 2 we show for different temperatures the fractions of u , d and s quarks, $Y_i = \rho_i/(N_c \rho)$, as a function of ρ , the total baryon density. It is clear the effect of temperature on the appearance of the quark s . We will see in section IV that the behavior of the bag pressure with density and temperature determines the onset of the mixed phase corresponding to the coexistence of hadron and quark matter.

III. HADRONIC MATTER EQUATION OF STATE

An extension of the NLWM [3] is the inclusion of the whole baryonic octet (n , p , Λ , Σ^+ , Σ^0 , Σ^- , Ξ^- , Ξ^0) in the place of the nucleonic sector. The presence of baryons heavier than the nucleons is expected in matter found in the core of neutron stars. The spin $\frac{3}{2}\Delta$ and the Ω^- hyperon should appear at even higher densities and hence are not included. The inclusion of other meson fields describing the $f_0(975)$ and $\phi(1020)$, which are a scalar and a vector meson field respectively is also important in reproducing the $\Lambda\Lambda$ interaction [18] but in this work we restrict ourselves to the most common σ , ω and ρ mesons.

The lagrangian density of the baryonic octet model (BOM) reads:

$$\mathcal{L}_{BOM} = \mathcal{L}_B + \mathcal{L}_{mesons} + \mathcal{L}_{leptons}, \quad (15)$$

where

$$\mathcal{L}_B = \sum_B \bar{\psi}_B [\gamma_\mu (i\partial^\mu - g_{\nu B} V^\mu - g_{\rho B} \mathbf{t} \cdot \mathbf{b}^\mu) - (M_B - g_{sB} \phi)] \psi_B,$$

with \sum_B extending over the eight baryons,

$$g_{sB} = x_{sB} g_s, \quad g_{vB} = x_{vB} g_v, \quad g_{\rho B} = x_{\rho B} g_\rho$$

and x_{sB} , x_{vB} and $x_{\rho B}$ are equal to 1 for the nucleons and acquire different values in different parametrizations for the other baryons,

$$\begin{aligned} \mathcal{L}_{mesons} = & \frac{1}{2}(\partial_\mu \phi \partial^\mu \phi - m_s^2 \phi^2) - \frac{1}{3!} \kappa \phi^3 - \frac{1}{4!} \lambda \phi^4 \\ & - \frac{1}{4} \Omega_{\mu\nu} \Omega^{\mu\nu} + \frac{1}{2} m_v^2 V_\mu V^\mu + \frac{1}{4!} \xi g_v^4 (V_\mu V^\mu)^2 \\ & - \frac{1}{4} \mathbf{B}_{\mu\nu} \cdot \mathbf{B}^{\mu\nu} + \frac{1}{2} m_\rho^2 \mathbf{b}_\mu \cdot \mathbf{b}^\mu, \end{aligned} \quad (16)$$

where $\Omega_{\mu\nu} = \partial_\mu V_\nu - \partial_\nu V_\mu$, $\mathbf{B}_{\mu\nu} = \partial_\mu \mathbf{b}_\nu - \partial_\nu \mathbf{b}_\mu - g_\rho (\mathbf{b}_\mu \times \mathbf{b}_\nu)$ and \mathbf{t} is the isospin operator.

In the above lagrangian, neither pions nor kaons are included because they vanish in the mean field approximation which is used in the present work and we do not consider the possible contribution of pion and kaon condensates. The electromagnetic field contribution also vanishes for homogeneous matter and its effect will not be taken into account in the mixed phase. Finally,

$$\mathcal{L}_{leptons} = \sum_l \bar{\psi}_l (i \gamma_\mu \partial^\mu - m_l) \psi_l. \quad (17)$$

In the mean field approximation, the meson equations of motion read:

$$\phi_0 = -\frac{\kappa}{2m_s^2} \phi_0^2 - \frac{\lambda}{6m_s^2} \phi_0^3 + \sum_B \frac{g_s}{m_s^2} x_{sB} \rho_{sB}, \quad (18)$$

$$V_0 = -\frac{\xi g_v^4}{6m_v^2} V_0^3 + \sum_B \frac{g_v}{m_v^2} x_{vB} \rho_B, \quad (19)$$

$$b_0 = \sum_B \frac{g_\rho}{m_\rho^2} x_{\rho B} t_{3B} \rho_B, \quad (20)$$

with

$$\rho_B = 2 \int \frac{d^3 p}{(2\pi)^3} (f_{B+} - f_{B-}), \quad (21)$$

$$\rho_{sB} = \frac{1}{\pi^2} \int p^2 dp \frac{M_B^*}{\sqrt{p^2 + M_B^{*2}}} (f_{B+} + f_{B-}),$$

with $M_B^* = M_B - g_{sB} \phi$, $E^*(\mathbf{p}) = \sqrt{\mathbf{p}^2 + M^{*2}}$ and $f_{B\pm} = 1/\{1 + \exp[(E^*(\mathbf{p}) \mp \nu_B)/T]\}$, where the effective chemical potential is $\nu_B = \mu_B - g_{vB} V_0 - g_{\rho B} t_{3B} b_0$.

The energy density in the mean field approximation reads:

$$\begin{aligned} \mathcal{E} = & 2 \sum_B \int \frac{d^3 p}{(2\pi)^3} \sqrt{\mathbf{p}^2 + M^{*2}} (f_{B+} + f_{B-}) + \\ & \frac{m_s^2}{2} \phi_0^2 + \frac{\kappa}{6} \phi_0^3 + \frac{\lambda}{24} \phi_0^4 + \frac{m_v^2}{2} V_0^2 + \frac{\xi g_v^4}{8} V_0^4 + \frac{m_\rho^2}{2} b_0^2 \\ & + 2 \sum_l \int \frac{d^3 p}{(2\pi)^3} \sqrt{\mathbf{p}^2 + m_l^2} (f_{l+} + f_{l-}), \end{aligned} \quad (22)$$

with the leptons distribution functions given after equation (14). The pressure becomes

$$\begin{aligned}
P = & \frac{1}{3\pi^2} \sum_B \int dp \frac{\mathbf{p}^4}{\sqrt{\mathbf{p}^2 + M^{*2}}} (f_{B+} + f_{B-}) \\
& - \frac{m_s^2}{2} \phi_0^2 - \frac{\kappa \phi_0^3}{6} - \frac{\lambda \phi_0^4}{24} + \frac{m_v^2}{2} V_0^2 + \frac{\xi g_v^4 V_0^4}{24} + \frac{m_\rho^2}{2} b_0^2 \\
& + \frac{1}{3\pi^2} \sum_l \int \frac{\mathbf{p}^4 dp}{\sqrt{\mathbf{p}^2 + m_l^2}} (f_{l+} + f_{l-}).
\end{aligned} \tag{23}$$

The expressions given in this section were obtained for finite temperature, but they can be trivially modified for $T = 0$ [19].

A. Hadronic matter in beta equilibrium

The condition of chemical equilibrium is also imposed through the two independent chemical potentials (μ_n and μ_e) and it implies that:

$$\mu_{\Sigma^0} = \mu_{\Xi^0} = \mu_{\Lambda} = \mu_n,$$

$$\mu_{\Sigma^-} = \mu_{\Xi^-} = \mu_n + \mu_e,$$

$$\mu_{\Sigma^+} = \mu_p = \mu_n - \mu_e.$$

For charge neutrality, we must have

$$\sum_B q_B \rho_B + \sum_l q_l \rho_l = 0, \tag{24}$$

where q_B and q_l stand respectively for the electric charges of baryons and leptons.

For the hadron phase we have used different parametrizations of the non-linear Walecka model. Two of them have been proposed to describe nuclei ground-state properties, NL3 [20] and TM1 [21], and a third parametrization GL (in the sequel) was proposed to describe the equation of state of neutron stars [5]. As shown in the expressions given above, the baryonic octet was included. In order to fix the meson-hyperon coupling constants we have used several choices discussed in the literature [5, 12]: a) according to [5, 22] we choose the hyperon coupling constants constrained by the binding of the Λ hyperon in nuclear matter, hypernuclear levels and neutron star masses ($x_\sigma = 0.7$ and $x_\omega = x_\rho = 0.783$) and assume that the couplings to the Σ and Ξ are equal to those of the Λ hyperon; b) we take $x_{sB} = x_{vB} = x_{\rho B} = \sqrt{2/3}$ as in [12, 23, 24, 25]. This choice is based on quark counting arguments; c) we consider $x_{sB} = x_{vB} = x_{\rho B} = 1$ known as universal coupling for comparison [26].

In the results we display, whenever $x_{sB} = x_{vB} = x_{\rho B}$, the unique coupling constant will be called x_H . We have checked that the parametrizations NL3 and TM1 become unstable respectively for $\rho/\rho_0 = 3.4$ and 6.5 if $x_H = \sqrt{2/3}$ and $\rho/\rho_0 = 3.5$ and 6.7 if $x_H = 1$ owing to the fact that nucleon mass goes to zero. The problem of the effective masses turning negative has been discussed in [27], and is due to the fact that the model includes baryons with different masses and different coupling constants to the σ field. This behavior is not exhibited if the hyperons are not included, when the effective mass of the nucleons decreases slowly with the density to zero at infinity. However, with the inclusion of the hyperons, and if the hyperon couplings are not chosen adequately [27], the σ field grows much faster with density. For this reason, we have chosen one of the parametrizations given in [5] (GL) in order to obtain the results for the mixed phase discussed in the next section. The chosen parameters are $g_s^2/m_s^2 = 11.79 \text{ fm}^2$, $g_v^2/m_v^2 = 7.148 \text{ fm}^2$, $g_\rho^2/m_\rho^2 = 4.41 \text{ fm}^2$, $\kappa/M = 0.005896$ and $\lambda = -0.0006426$, for which the binding energy is -16.3 MeV at the saturation density $\rho_0 = 0.153 \text{ fm}^{-3}$, the symmetry coefficient is 32.5 MeV , the compression modulus is 300 MeV and the effective mass is $0.7M$, higher than in the other two parametrizations.

In reference [18], the authors have imposed a positive value for the effective mass by taking its modulus and ignoring the fact that it becomes zero and then negative. This gave rise to discontinuities in their figures for some of the parametrizations used. For the TM1 parameter set, there are no discontinuities, but in their model they include other mesons than the σ, ω and ρ , and the behavior of the effective mass also depends on the hyperon-meson coupling constants used. In [13] the authors also claim to have used the TM1 parametrization in order to study the mixed stars, but since no data are given for this parameter set we believe it has only been used for stars with no phase transition to the quark phase.

IV. MIXED PHASE

In the mixed phase charge neutrality is not imposed locally but only globally, as mentioned in the introduction [5, 13]. This means that the quark and hadronic phases are not neutral separately, but rather, the system will prefer to rearrange itself so that

$$\chi \rho_c^{QP} + (1 - \chi) \rho_c^{HP} + \rho_c^l = 0,$$

where ρ_c^{iP} is the charge density of the phase i , χ is the volume fraction occupied by the quark phase, $(1 - \chi)$ is the volume fraction occupied by the hadron phase and ρ_c^l is the electric charge density of leptons. We consider a uniform background of leptons in the mixed phase since Coulomb interaction has not been taken into account. According to the Gibb's conditions for phase coexistence, the baryon chemical potentials, temperatures and pressures have to be identical in both phases, i.e.,

$$\mu_{HP} = \mu_{QP},$$

$$T_{HP} = T_{QP},$$

$$P_{HP}(\mu_{HP}, T) = P_{QP}(\mu_{QP}, T),$$

reflecting the needs of chemical, thermal and mechanical equilibrium, respectively. As a consequence, the energy density and total baryon density in the mixed phase read:

$$\langle \mathcal{E} \rangle = \chi \mathcal{E}^{QP} + (1 - \chi) \mathcal{E}^{HP} + \mathcal{E}^l \quad (25)$$

and

$$\langle \rho \rangle = \chi \rho^{QP} + (1 - \chi) \rho^{HP}. \quad (26)$$

At this point the EOS in the mixed phase has to be built. In this work we use for the hadronic phase the parametrization corresponding to $K = 300$ MeV and $M^*/M = 0.7$ displayed in the previous section. It predicts a mixed phase in a range of densities which depends on the model used for the quark phase and on the hyperon coupling constants. The higher the hyperon couplings and the compressibility and the lower the effective mass the lower lies the range of densities corresponding to the mixed phase. This has already been discussed in [5, 12]. For the quark phase we consider both the NJL model and the MIT Bag model with two different bag pressures, as mentioned in section II. The choice of the bag pressures was done in such a way that for the lower value, $B^{1/4} = 180$ MeV, the onset of a quark-hadron mixed phase occurs before the appearance of hyperons, and for $B^{1/4} = 190$ MeV the hyperons appear before the quarks. With the present study we have concluded that the existence of a quark phase, and a mixed phase is very sensitive to the choice of the hyperon couplings. For a quark phase described by the NJL model the mixed/quark phase only exists if the $\Lambda - \sigma$ coupling is not very weak, namely $x_\sigma \geq 0.65$ with the other hyperon coupling constants constrained by the binding of the Lambda hyperon in nuclear matter. This can be understood in the following way: there will be a quark component only if its effect is to soften the EOS. Large hyperon couplings mean that the hadronic EOS becomes harder since at high densities the EOS is dominated by the repulsion described by the vector mesons. Therefore a transition to a quark phase may be favorable if it softens the EOS. A weaker x_σ than a x_ω also favors the phase transition for the same reason, i.e., it gives rise to a harder EOS.

In fig 3 we plot the hadronic EOS obtained for several hyperon couplings and the NJL EOS as a function of the neutron chemical potential μ_n . For the hyperon couplings we have considered besides the couplings already introduced in the present paper, two other sets, both constrained by the Λ hyperon binding to nuclear matter [5], with $x_\sigma = 0.6$ and 0.8. For the first value of x_σ we do not get a phase transition to quark matter with the NJL model. The value $x_\sigma = 0.8$ was chosen in ref. [14], but according to [5] could be a bit too high if we consider hypernuclear levels which give an uncertain upper bound of $x_\sigma = 0.72$. The EOS with $x_H=1$. is very similar to the one obtained with $x_\sigma = 0.7$, $x_\omega = x_\rho = 0.783$. We have assumed that the couplings to the Σ and Ξ hyperons are equal to those of the Λ hyperon. However, we have also tested that if we had taken for the Σ couplings the two different sets proposed in [27], which give satisfactory fits to the Σ^- atom ($x_{\sigma\Sigma} = 0.77$, $x_{\omega\Sigma} = 1.$, $x_{\rho\Sigma} = 0.67$ or $x_{\sigma\Sigma} = 0.54$, $x_{\omega\Sigma} = 0.67$, $x_{\rho\Sigma} = 0.67$) the densities corresponding to the onset of the mixed phase and the pure quark matter phase would not alter.

According to [2] for a newborn neutron star the entropy per baryon across the star is approximately constant, of the order 1 to 2. This corresponds to temperatures which can go up to 30 MeV [1, 2]. In fig 4 we plot the entropy for different temperatures obtained with the NJL model. We conclude that, except, for a small effect in the mixed

phase, in the interior of the star ($\rho > 2\rho_0$) the entropy does not change with temperature. Exactly the same trend is observed with the Bag model. Therefore, we use the EOS obtained for different parametrizations at fixed temperatures to determine the properties of proto-neutron stars, and we are confident that there will not be big differences for not using fixed entropies.

The rise of the entropy in the mixed phase corresponds to a decrease in temperature in the interior of the star, if a fixed entropy calculation were performed. This effect has also been discussed in ref. [14] and it is due to the opening of new degrees of freedom in the system. Similar results were obtained with the Bag model.

In order to implement both phases in a common code, we have imposed the Gibb's conditions and rewritten the quark chemical potentials of equations (13) in terms of the electron and neutron chemical potentials, i.e.,

$$\mu_u = (\mu_n - 2\mu_e)/3 \quad \mu_d = \mu_s = (\mu_n + \mu_e)/3.$$

Examples of the particle populations obtained from the construction of the full EOS are shown in figures 6 and 7. Notice that if the Bag model is used, the quarks appear at relatively low densities, sometimes lower than the densities for which some of the hyperons turn up, depending on the value of *Bag*. This behavior was also observed in [1, 5]. If the NJL model is used the appearance of the quarks depends very much on the hyperon coupling constants. Two different behaviors were obtained: a) the hyperons appear before the quarks and the mixed phase occurs at much higher densities, ($\sim 5\rho_0$); b) the quarks appear at $T = 0$ at lower densities than the hyperons if the effective bag pressure at the onset of the mixed phase is still well below the plateau around 162 MeV. In this second case the phase transition occurs at $\sim 2\rho_0$ and the effective bag pressure increases to its plateau value for densities inside the mixed phase. This gives rise to several effects such as a plateau on the quark content after the initial increase as can be observed in figure 7 at $T = 0$. For $T > 10$ MeV this last effect disappears because the rise of the effective bag pressure occurs at higher densities. With this set of hyperon couplings there is a transition with temperature: for $T = 0$ MeV the quarks appear before the hyperons, at $T = 5$ MeV both appear at a similar density; for higher temperatures the hyperons appear at lower densities. One main difference between the Bag model and the NJL model predictions is the relative fractions of *u*, *d*, and *s* quarks: in the Bag model all the three types of quarks appear at a similar density, then the fraction of *d* and *s* quarks increases faster and only close to the onset of the pure quark matter the *u* fraction becomes larger than the *s* quark fraction. At these densities, however, the *u*, *d*, *s* quark fractions are very close to each other, of the order ~ 0.33 . With the NJL model the *d* quark appears first, at a higher density the *u* quark appears and still higher the *s* quark turns up. The *d* (*s*) quark fraction is always the largest (lowest). Only at very high densities, well inside the pure quark matter phase, do all three quark fractions get close to 0.33. These behavior is due to the fact that in the NJL model, only at quite large densities the mass of the *s* quark gets close to its current mass value.

For all EOS obtained the higher the temperature, the lower the densities for which the hyperons appear. The onset of the mixed phase occurs in most cases studied at higher densities for a higher temperature, the exception being the the NJL model for $x_H = \sqrt{2/3}$. This can be confirmed in Fig. 5 where the full EOS, obtained respectively with the Bag and the NJL models, for $x_H = \sqrt{2/3}$, are given for different temperatures. For this choice of hyperon couplings the Bag model predicts a mixed phase at lower densities (energies). For the other two choices of hyperon couplings studied with the NJL model, the mixed phase occurs before the effective bag pressure reaches the 163 MeV plateau, and this dictates the difference. For $x_s = 0.7$ and $x_H = 1.0$ the onset of the mixed phase is determined by the low density behavior of the NJL EOS. As discussed in [28], the EOS obtained within this parametrization of NJL model contains mechanical unstable regions which give the possibility of a first-order phase transition of the liquid-gas type. Depending on the set of hyperon couplings chosen, it can happen that the mixed phase appears precisely at the density above which the NJL is stable against density and charge fluctuations.

The presence of strangeness in the core and crust of neutron and proto-neutron stars can have important consequences in understanding some of their properties [29, 30, 31, 32]. We have calculated the strangeness content of the different EOS as a function of density. In figures 8 and 9 we plot the strangeness fraction r_s defined as

$$r_s = \chi r_s^{QP} + (1 - \chi) r_s^{HP} \tag{27}$$

with

$$r_s^{QP} = \frac{\rho_s}{3\rho}, \quad r_s^{HP} = \frac{\sum_B |q_s^B| \rho_B}{3\rho},$$

where q_s^B is the strange charge of baryon *B*. When the quark phase is described by the Bag model the strangeness fraction rises steadily and at the onset of the quark phase it has almost reached 1/3 of the baryonic matter. This behavior is independent of the hyperon-meson coupling constants used in this work. The NJL model predicts a different behavior: in the mixed phase the strangeness fraction decreases and increases again for pure quark matter.

This behavior is due to fact that for the densities at which the mixed phase occurs the mass of the strange quark is still very high. The overall effect of temperature is to increase the strangeness fraction, except for the mixed phase with the NJL model where the strangeness fraction decreases more strongly for higher temperatures.

V. MIXED STAR PROPERTIES

In the present section we investigate the properties of stellar objects formed by matter described by the EOS studied in the previous sections. Mixed proto-neutron and neutron star profiles can be obtained from all the EOS studied by solving the Tolman-Oppenheimer-Volkoff (TOV) equations [33], resulting from a simplification of Einstein's general relativity equations for spherically symmetric and static stars. For a certain EOS the TOV equations for pressure and mass are integrated from the origin for a set of arbitrary choices for the the central density, in such a way that they define a one-parameter family of stars. The neutron star mass is an increasing function of its central density until it reaches a maximum, where matter can collapse to a black hole. It means that the values of the maximum mass of a star is very important in the determination of the mass of possible black holes. The Oppenheimer-Volkoff limit gives the maximum value of the neutron star mass. There are theoretical previsions that the maximum mass varies from 0.72 solar mass (M_\odot) obtained for pure neutron matter stars up to $3.26 M_\odot$ [34]. Other authors [25], based on recent calculations, claim that they can be in the interval $1.6 M_\odot$ and $2.1 M_\odot$. According to [5], the observed values lie between $1.2 M_\odot$ and $1.8 M_\odot$.

In tables 1 and 2 we show the values obtained for the maximum mass of a neutron star as function of the central density for some of the EOS studied in this work and for different temperatures. In table 1 the GL force and the NJL model were used to derive the full EOS, while in table 2 the EOS was obtained from the GL force and the MIT Bag model. Several conclusions can be drawn. For all EOS studied, the central energy density ε_0 falls inside the mixed phase. In some cases, at finite temperature, it can even occur in the quark phase. This happens in the calculation with NJL if the universal coupling is chosen and in the calculation with the Bag model with $B^{1/4} = 180$ MeV. Similar results were obtained in [14]. However, the present results are different from the ones discussed in [13], where the parametrization of the EOS used allowed for the appearance of the mixed phase only in a quite narrow mass range. The maximum masses of the stars do not show any regular behavior with temperature, contrary to the steady increase of the maximum allowed mass obtained with the GL model alone as shown in table 3. It is worth emphasizing that the EOS for $T=0$ and $T=10$ MeV are very close to each other (at least for GL plus Bag models), what could have led to very small differences in the solutions of the TOV equations. The trend seems to be a small decrease at lower temperatures followed by a small increase. Only in one case we have obtained a continuous increase of the mass. A discussion of the possibility of a back hole formation after the deleptonization and cooling of the proto-neutron star requires a more careful study. In principle, this could happen if the maximum allowed mass at $T = 0$ MeV is lower than the maximum allowed mass at finite T .

Comparing tables 1 and 2 we conclude that the Bag model allows for smaller maximum masses, of the order $\sim 1.6 M_\odot$, than the NJL model, $\sim 1.9 M_\odot$. Several quite high mass limits have been recently determined [35, 36] which could rule out soft EOS with phase transition to deconfined matter. In particular, the determination of the pulsar Vela X-1 gives the mass $M_X = 1.86 \pm 0.16 M_\odot$. However, these high mass limits do not exclude a phase transition to quark matter within the NJL model. It is also seen that the maximum mass does not depend much on the hyperon couplings although in the NJL the same is not true for the onset of the mixed phase. For comparison we show in table 3 the properties of stars obtained with the GL model (transition to the quark phase not included). While the maximum masses obtained with Bag model are ~ 15 % smaller than with the hadron EOS, the ones obtained within the NJL model are only ~ 3 % smaller.

We will not discuss the radius of the maximum mass star because it is sensitive to the low density EOS and we did not describe properly this range of energy densities.

VI. CONCLUSIONS

In the present paper we have studied the EOS for proto-neutron stars using both the Bag model and the NJL model for describing the quark phase and a relativistic mean-field description in which baryons interact via the exchange of σ -, ω -, ρ - mesons for the hadron phase. Parametrizations TM1 and NL3 fitted to the ground-state properties of stable and unstable nuclei proved to be inadequate because, due to the inclusion of hyperons, the nucleon mass becomes negative at relatively low densities. We have considered a parametrization which describes the properties of saturating nuclear matter proposed in [5]. For the hyperon couplings we have used three choices and verified that for the NJL model the onset of the mixed phase is sensitive to the hyperon couplings. We have verified that the choice

of other sets of hyperon couplings, namely couplings to the Σ and Ξ different from the Λ hyperon, did not have any effect on the onset of the mixed phase.

If the quark phase is described by the Bag model the strangeness content of the EOS rises steadily and at the onset of the quark phase it has almost reached 1/3 of the baryonic matter. However, the NJL model predicts a different behavior: in the mixed phase the strangeness fraction decreases and increases again for pure quark matter. The overall effect of temperature is to increase the strangeness fraction, except for the mixed phase with the NJL model where the strangeness fraction decreases more strongly for higher temperatures. The strangeness content will influence the cooling rates of the star [31, 32].

The consequences of using a model with chiral symmetry have been discussed. The onset of the mixed phase is the result of a delicate equilibrium between the hyperon couplings and the rise of the effective bag pressure due to partial restoration of the chiral symmetry. The value of the effective bag pressure also dictates whether the onset of hyperons occurs at larger or lower densities than the onset of the mixed phase. Temperature will alter the order if at $T = 0$ MeV the onset of the mixed phase occurs at lower densities. A large s quark mass until very high density gives rise to a decrease of the strangeness content of the EOS in the mixed phase. In the quark phase the fraction of the s quark becomes similar to the d and u quark fractions at densities greater than $10 \rho_0$.

The appearance of the mixed phase in β -equilibrium matter at a fixed temperature gives rise to an increase of the entropy per baryon due to the opening of other allowed channels. This will affect neutrino-matter interaction rates [31].

With the EOS studied in the present work, the mixed stars obtained from the integration of the TOV equations contain a core constituted by a mixed phase. Only in very special cases, a small core of pure quark matter exists. It was shown that the maximum masses of mixed stars obtained with the Bag model are of the order of $\sim 1.6 M_\odot$, smaller than the maximum masses obtained within the NJL model, $\sim 1.9 M_\odot$. Even with a transition to a deconfinement phase the masses predicted can be quite high. Maximum masses for neutron stars obtained in the present work are larger than the ones obtained in [1]. The effect of temperature in the maximum masses allowed is not strong. The central energy densities, though, decrease with temperature.

We are aware of the importance of neutrino trapping in the description of proto-neutron star properties and this feature will be incorporated in a forthcoming work. The effects arising from the inclusion of pion and kaon condensates seem not to be very large and also very dependent of the choice of the hyperon to meson coupling constants [1, 5], which are not known quantities. For these reasons they were not incorporated in this study. Some authors [18, 37] have claimed that other meson fields, namely the scalar meson field $f_0(975)$ and the vector meson field $\phi(1020)$, should also be incorporated in order to reproduce the observed strongly attractive $\Lambda\Lambda$ interaction. We believe that the inclusion of these meson fields will not have a great influence on the properties of the stars under consideration. It is well known that non-rotating neutron stars are practically undetectable. The extension of this work in order to include the rotation mechanism discussed in [5, 35] is under consideration.

Moreover, the quark-meson coupling model (QMC) [38], which describes nuclear matter as a system of non-overlapping MIT Bags which interact through the effective scalar and vector mean fields, is also a good option for the description of the hadron phase. The quark phase appears naturally as the breakdown of the confining bags takes place. This investigation is also under way. In the present work we have only considered unpaired quark matter. However, recent studies seem to show that the quark phase, if present, would be in a color superconductor phase [39, 40]. The possible existence of a color superconductor quark phase in compact stars has been studied in references [41] with the Bag model and [42] using the NJL model. In general, it was shown that the inclusion of a color superconductor phase would soften the EOS at lower pressures giving rise to the onset of quarks, either through a sharp transition or a mixed phase, at lower densities. With the NJL model and a sharp transition assumption no stable stars with a quark core were found. Properties of compact stars obtained within the Bag model depend on the parameter set used and the sharp/mixed transition considered, but it was shown that color superconductivity could boost the mass of the star. Further studies on the possible existence and consequences of a color superconductor phase are still needed.

ACKNOWLEDGMENTS

We would like to acknowledge fruitful discussions with Célia Sousa and Marcelo Chiapparini. This work was partially supported by CNPq (Brazil), CAPES(Brazil)/GRICES (Portugal) under project 003/100 and FEDER/FCT

(Portugal) under the project . POCTI/35308/FIS/2000.

-
- [1] M. Prakash, I. Bombaci, M. Prakash, P. J. Ellis, J. M. Lattimer and R. Knorren, Phys. Rep. 280, 1 (1997).
 - [2] A. Burrows, J.M. Lattimer, Astroph. J. 307 (1986) 178.
 - [3] B.D. Serot and J.D. Walecka, Adv. Nucl. Phys. **16** (1986) 1.
 - [4] J. Boguta and A. R. Bodmer, Nucl. Phys. **A292** (1977) 413.
 - [5] N. K. Glendenning, Compact Stars, Springer-Verlag, New-York, 2000.
 - [6] A. Chodos, R.L. Jaffe, K. Johnson, C.B. Thorne and V.F. Weisskopf, Phys. Rev. **D 9** (1974) 3471.
 - [7] Y. Nambu and G. Jona-Lasinio, Phys. Rev. **122** (1961) 345; **124** (1961) 246.
 - [8] S. P. Klevansky, Rev. Mod. Phys. 64 (1992) 649; P. Zuang, J. Hüfner and S. P. Klevansky, Nucl. Phys. A 576 (1994) 525.
 - [9] T.Hatsuda and T. Kunihiro, Phys. Rep. 247 (1994) 221.
 - [10] J. da Providência, M. C. Ruivo and C. A. de Sousa, Phys. Rev. D 36 (1987) 1882; C. A. de Sousa, Z. Phys. C 8s 43 (1989) 503; M. C. Ruivo, C. A. de Sousa, B. Hiller and A. H.Blin, Nucl. Phys. A 575 (1994) 460.
 - [11] C. Ruivo, C. Sousa e C. Providência, Nucl. Phys. A 651 (1999) 59; Pedro F. S. Costa, Master Thesis, 2001.
 - [12] S. K. Ghosh, S. C. Phatak and P. K. Sahu, Z. Phys. **A 352** (1995) 457.
 - [13] K. Schertler, S. Leupold and J. Schaffner-Bielich, Phys. Rev c **60**, 025801 (1999).
 - [14] A. W. Steiner, M. Prakash and J. M. Lattimer, Phys. Lett. B **486** (2000) 239.
 - [15] T. Kunihiro, Phys. Lett. **B 219**, 363 (1989).
 - [16] P. Rehberg, S. P. Klevansky, and J. Hüfner, Phys. Rev. C **53**, 410 (1996).
 - [17] M. Buballa and M. Oertel, Phys. Lett. B **457**, 261 (1999).
 - [18] J. Schaffner and I. Mishustin, Phys. Rev. **C 53** (1996) 1416.
 - [19] A.L. Espíndola and D.P. Menezes, Phys. Rev. **C 65** (2002) 045803.
 - [20] G. A. Lalazissis, J. König and P. Ring, Phys. Rev. **C 55** (1997) 540.
 - [21] K. Sumiyoshi, H. Kuwabara, H. Toki, Nucl. Phys. **A 581** (1995) 725.
 - [22] N. K. Glendenning and S. Moszkowski, Phys. Rev. Lett. **67**, 2414 (1991).
 - [23] S.A. Moszkowski, Phys. Rev. **D 9** (1974) 1613.
 - [24] N. K. Glendenning, Nucl. Phys. **A 493** (1989) 521.
 - [25] A.R. Taurines, C.A.Z. Vasconcelos, M. Malheiro and M. Chiapparini, Phys. Rev. **C 60**, 065801 (1999).
 - [26] N. K. Glendenning, Astrophys. J. **293**, 470 (1985).
 - [27] R. Knorren, M. Prakash and P. J. Ellis, Phys. Rev. C **52**, 3470 (1995).
 - [28] M. Hanauske, L. M. Satarov, I. N. Mishustin, H. Stöcker, and W. Greiner, Phys. Rev. D **64**, 043005 (2001).
 - [29] C. Alcock, E. Farhi and A. Olinto, Astrophys. J. 310 (1986) 261.
 - [30] S. Balberg, I. Lichtenstadt and G. B. Cook, Astrophys. J. Suppl. **121**, 515 (1999).
 - [31] S. Reddy, M. Prakash and M. Lattimer, Phys. Rev. D **58**, 013009 (1998).
 - [32] J. A. Pons, S. Reddy, M. Prakash, J. M. Lattimer, and J. A. Miralles, Astrophys. J. **513**, 780 (2001).
 - [33] R.C. Tolman, Phys. Rev. **55** (1939) 364; J.R. Oppenheimer and G.M. Volkoff, Phys. Rev. **55** (1939) 374.
 - [34] K.C. Chung, *Vamos falar de estrelas?*, Rio de Janeiro, 2000 - Edição do autor.
 - [35] H. Heiselberg and M. Hjorth-Jensen, Phys. Rep. **328**, 237 (2000).
 - [36] Barziv, O.; Kaper, L.; Van Kerkwijk, M. H.; Telting, J. H.; Van Paradijs, J, A&A.**377**, .925 (2001).
 - [37] S. Pal, M. Hanauske, I. Zakout, H. Stöcker and W. Greiner, Phys. Rev. **C 60**, 015802 (1999).
 - [38] P. A. M. Guichon, Phys. Lett. **B200**, 235 (1988); K. Saito and A.W. Thomas, Phys. Lett. **B327**, 9 (1994).
 - [39] R. Rapp, T. Schäfer, E. V. Shuryak and M. Velkovsky, Ann. Phys. (N.Y.) **280**, 35 (2000); M. Alford, Ann. Rev. Nucl. Part. Sci. 51, **131** (2001).
 - [40] A. W. Steiner, S. Reddy, and M. Prakash, Phys. Rev. **D 66**, 094007 (2002); M. Buballa, M. Oertel, Nucl. Phys. **A703**, 770 (2002); F. Neumann, M. Buballa, M. Oertel, Nucl. Phys. **A714**, 481 (2003).
 - [41] M. Alford and S. Reddy, Phys. Rev. **D 67**, 074024 (2003)
 - [42] M. Baldo, M. Buballa, G.F. Burgio, F. Neumann, M. Oertel, H.-J. Schulze, Phys. Lett. **B562**, 153 (2003)

Table 1 - Mixed star properties for the EOS obtained with the GL force and the NJL model.

	T (MeV)	M_{\max}/M_{\odot}	ε_0 (fm $^{-4}$)	ε_{min} (fm $^{-4}$)	ε_{max} (fm $^{-4}$)
$x_H = \sqrt{2/3}$	0	1.84	6.29	4.60	7.25
	10	1.83	6.34	4.58	7.14
	20	1.84	6.26	4.50	6.66
	30	1.85	5.85	4.23	5.84
$x_s = 0.7$	0	1.90	5.01	1.30	5.21
	10	1.89	4.98	1.31	5.13
$x_{\omega} = 0.783$	20	1.89	4.81	1.37	4.82
	30	1.90	4.34	1.61	4.44
$x_H = 1.$	0	1.92	5.08	1.30	5.22
	10.	1.89	5.13	1.54	5.10
	20	1.88	4.92	2.20	4.83
	30	1.87	4.58	2.18	4.46

Table 2 - Mixed star properties for the EOS obtained with the GL force and the MIT Bag model.

	T (MeV)	M_{\max}/M_{\odot}	ε_0 (fm $^{-4}$)	ε_{min} (fm $^{-4}$)	ε_{max} (fm $^{-4}$)	
Bag $^{1/4}$ =180 MeV	0	1.40	7.38	1.17	4.62	
	$x_H = \sqrt{2/3}$	10	1.39	7.05	1.17	4.58
		20	1.42	4.18	1.20	4.47
Bag $^{1/4}$ =190 MeV	0	1.64	4.58	1.81	6.06	
	$x_H = \sqrt{2/3}$	10	1.59	4.86	1.85	6.03
		20	1.67	4.18	1.90	5.93
		30	1.76	3.18	1.96	5.78
$x_s = 0.7$	0	1.63	4.43	1.53	6.0	
	10	1.63	4.41	1.57	5.95	
$x_{\omega} = 0.783$	20	1.63	4.10	1.62	5.86	
	30	1.64	3.82	1.67	5.69	
$x_H = 1$	0	1.64	4.49	1.63	6.01	
	10	1.65	4.40	1.66	5.98	
	20	1.67	4.12	1.71	5.87	
	30	1.72	3.61	1.76	5.70	

Table 3 - Compact star properties for the EOS obtained with the GL force

	T (MeV)	M_{\max}/M_{\odot}	ε_0 (fm $^{-4}$)
$x_H = \sqrt{2/3}$	0	1.93	6.36
	10	1.93	6.34
	20	1.95	6.20
	30	1.97	5.85

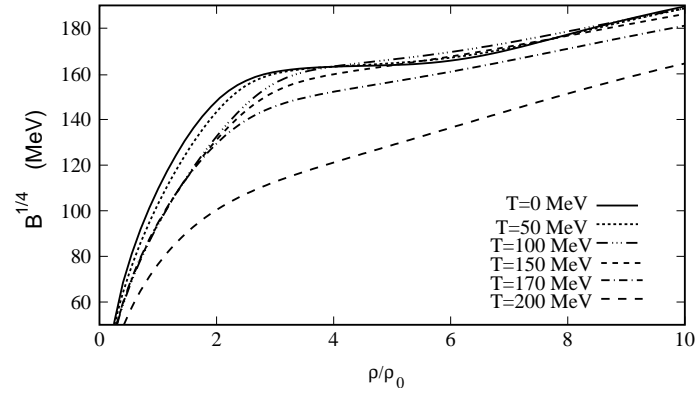


FIG. 1: NJL model in beta equilibrium: the bag effective pressure at different temperatures

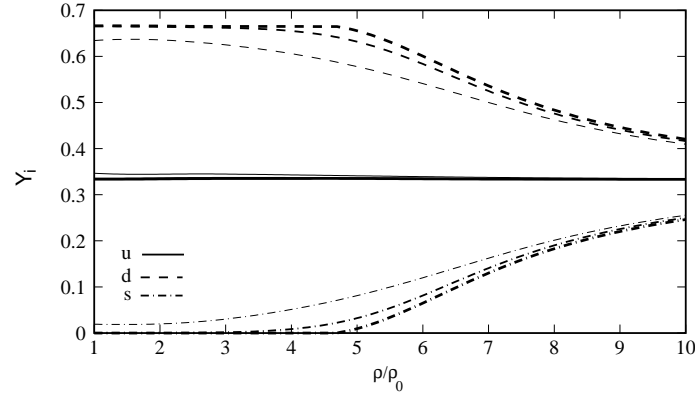


FIG. 2: The fraction of quarks u,d,s in beta equilibrium at $T=0, 20$ and 50 MeV (from very thick to thin)

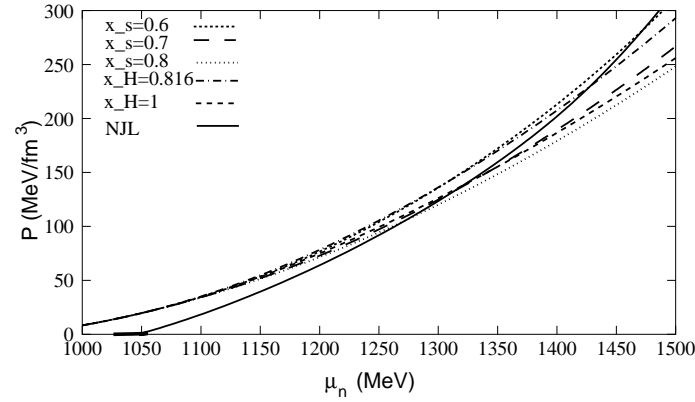


FIG. 3: The EOS for the NJL model and for GL model with different choices of the hyperon couplings)

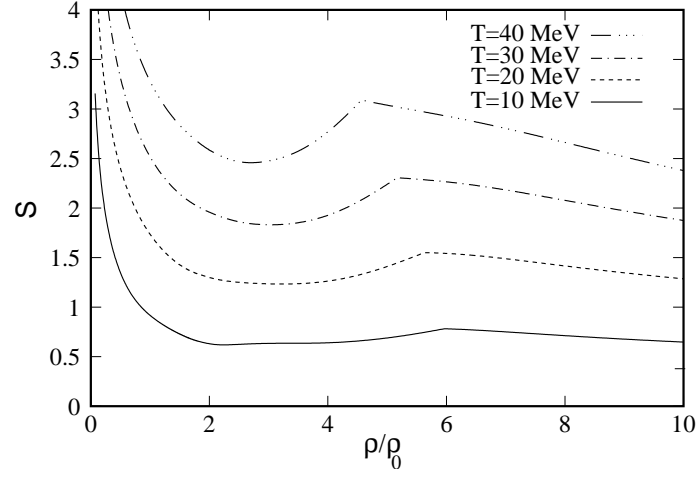


FIG. 4: Entropy per baryon for different temperatures. The quark phase is described by the NJL model.

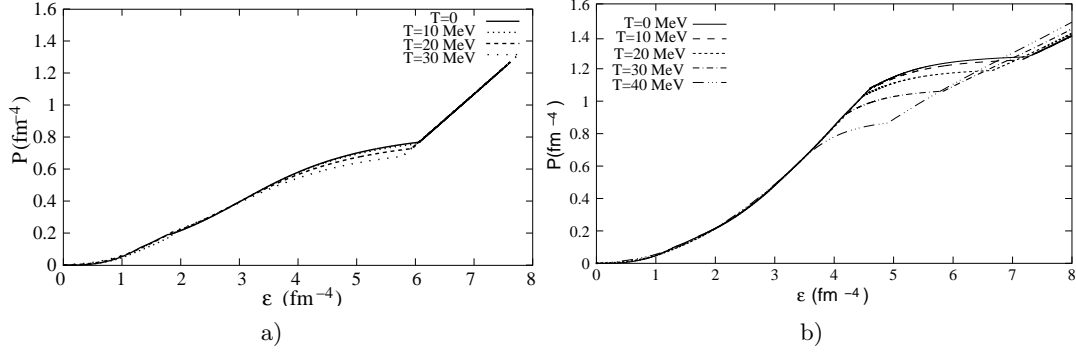


FIG. 5: EOS obtained with the GL force plus a) Bag model for $\text{Bag}^{1/4}=190$ MeV; b) NJL model. In both cases $x_H = \sqrt{2/3}$.

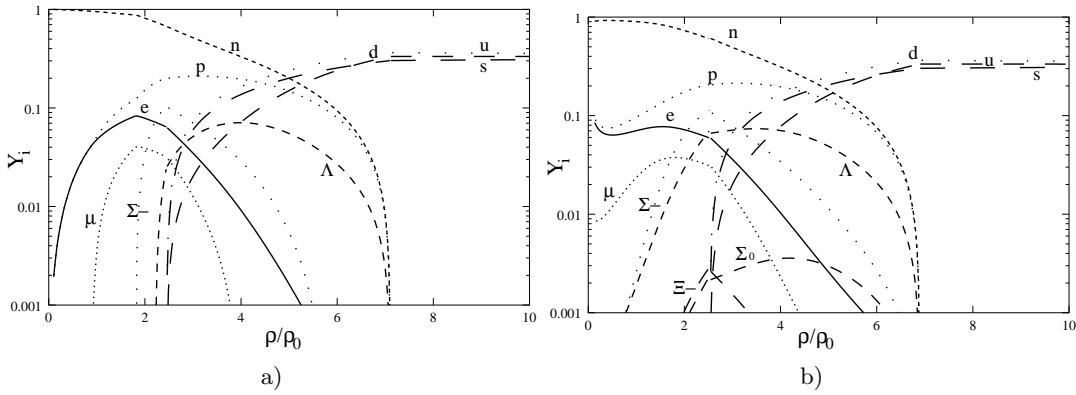


FIG. 6: Particle fractions $Y_i = \rho_i/\rho$, for $i =$ baryons, leptons and quarks, obtained with the GL force plus the Bag model for $\text{Bag}^{1/4}=190$ MeV and a) $T=0$ b) $T=20$ MeV. In both cases $x_H = \sqrt{2/3}$.

